A NUMERICAL APPROACH TO IDENTIFY INJURY RISK REGIONS WITHIN SOFT TISSUES OF DYNAMIC HUMAN BODY FINITE ELEMENT MODELS

James Gaewsky
Derek Jones
Ashley Weaver
Joel Stitzel
Wake Forest School of Medicine
United States

Paper Number 17-0057

ABSTRACT

Objective: As different morphologies and postures of human body models (HBMs) are developed, simulations of occupants in real world motor vehicle collisions (MVCs) can become more sensitive to injury risk factors. Despite the detail of modern HBMs, most dynamic analyses of these models studied body region-level injury metrics like displacements and accelerations, while most element-level analyses focus on peak stresses and strains. The objective of this study was to analyze the dynamic nature of thoracic soft tissue deformations using local areas of increased strains to identify potential injury sites.

Methods: Eleven frontal MVCs from the CIREN and NASS-CDS databases were reconstructed using a previously developed dynamic finite element methodology. These MVC reconstructions used scaled versions of the Total HUman Model for Safety (THUMS) AM50 v4.01 and a tuned simplified vehicle model. CIREN radiology and NASS-CDS injury reports indicated that five of eleven driver occupants sustained soft tissue thoracic injuries (AIS 2+) including pulmonary contusion, pneumothorax, hemothorax, and hemomediastinum. In each simulation, strain data were output for all elements in the lungs, pleurae, heart, pericardium, and rib cage at 0.5 ms intervals. The shape of the time-varying profiles of each element for maximum principal strain (ε_{mp}) were compared using normalized cross-correlation. The normalized cross-correlation coefficient between each pair of elements allowed grouping of elements that shared similar time-dependent deformation patterns during the impact. Element groups with increased strain metrics were identified as hotspots.

Results: The dynamic deformation profiles for each anatomical structure were processed for each reconstructed MVC. A fraction of elements exceeding previous pulmonary contusion strain thresholds were calculated. The largest hotspot's average ε_{mp} for the left lung ($p=0.43$), right lung ($p=0.70$) and heart ($p=0.76$) parts were not significantly different between injurious and non-injurious cases.

Conclusions: A method to analyze dynamic deformation patterns in FE simulations was applied across eleven MVC reconstructions. This algorithm promotes understanding which regions of the anatomical structures deform together, and may improve the ability to model complex and multiphasic injury mechanisms.

INTRODUCTION

Modern computational human body models (HBMs) have been developed and validated to understand common blunt trauma injuries and mechanisms. The Total Human Model for Safety (THUMS) v4.01 is a HBM that includes geometric and mechanical detail of the head and brain, bones of the trunk and limbs, and thoraco-abdominal organs. The response of each body region and organ in HBM simulations represents a unique challenge to numerically model the associated injury outcomes.

In motor vehicle crashes (MVCs), thoracic injuries rank second in terms of the body region most frequently injured, severity, and overall economic and social cost [1, 2]. Thoracic blunt trauma injuries can be broadly grouped in two categories: 1) bony or rib fracture injuries and 2) soft tissue injuries [3, 4]. While these two injury modes are often inter-related and can be concurrently estimated based on correlative injury metrics including chest deflection, force or acceleration, they can also be characterized by the specific associated mechanical insult [5-7].

While there is a wealth of data related to bony thoracic injuries in HBMs, there is less existing literature related to prediction of the most common thoracic soft tissue injury models in computational models. One of the unique challenges with respect to modeling soft tissue thoracic injuries in finite element models (FEMs) is that these injuries are often identified by their physiologic response rather than a mechanical failure [3]. For example, pulmonary contusion (PC) is primarily characterized by the inflammatory response and edema buildup within the lungs, while hemothorax and pneumothorax injuries are characterized by collection of blood or air in the pleural space [8, 9]. Previous authors have correlated finite element-based strain metrics to PC, in rat models and reconstructions of side impact real world MVCs [10-12]. These studies measured the segmented volumes of lung tissue with edema (representing PC) in computed tomography (CT) scans. In FEM reconstructions of the injury events, the threshold value of each strain based metric, including maximum principal strain (ε_{max}), corresponding to the injured tissue volume were identified.

However these PC injury metrics and evaluation methods may not adequately characterize the dynamic behavior of the soft tissue response in a fashion that is necessary to quantify PC or several other thoracic soft tissue injuries. One shortcoming of the PC element volume analysis method is related to the temporal response of the injured tissue. After a crash event occurs, the region of tissue with a strong inflammatory response may not be the same as the tissue regions that experienced the greatest deformations [13]. Additionally, the medical and biomechanics communities would benefit from modeling several other of the most common blunt chest trauma injuries that are characterized by more focal mechanical insults. Injuries including hemomediastinum, hemothorax, and pneumothorax are often a result of more focal trauma where localized interaction with fractured ribs or other brief, increased deformations patterns occur [3]. To analyze these injuries in a FEM, it may be more important to identify local deformation hotspots within a part with differing deformation patterns from their neighboring elements.

The objective of this study was to analyze the dynamic response behavior of thoracic soft tissue to promote further validation of crash induced injuries (CII) and mechanisms in HBMs by leveraging existing real world MVC data. Based on the analysis of the dynamic soft tissue responses in 11 MVC reconstruction simulations in this study – five with Abbreviated Injury Scale (AIS) 2+ thoracic soft tissue injuries, and six without – algorithms to identify regions with elevated risks of injury in specific thoracic tissues and organ models were developed. This study evaluated deformation metrics primarily related to the pulmonary and cardiac tissues.

METHODS

Reconstruction Case Selection

A total of 11 real-world MVCs, documented in either the Crash Injury Research and Engineering Network (CIREN) or National Automotive Sampling System-Crashworthiness Data System (NASS-CDS) databases, were reconstructed using dynamic FEMs. Each full frontal, planar MVC reconstruction case was selected using the criteria described by Gaewsky et al. [14]. While all 11 occupants had at least one AIS 2+ injury, only five of the 11 occupants sustained AIS 2+ injuries to soft tissue organs in the thoracic cavity. The 11 occupants were split into "injury" and "non-injury" categories based on the presence of AIS 2+ soft tissue thoracic injury. The vehicle and occupant characteristics and injury outcomes for the 11 case reconstructions are summarized in Table 1.

Case Reconstruction Process

Each MVC reconstruction was performed using the Total Human Model for Safety (THUMS) version 4.01 and a simplified vehicle model (SVM) as previously validated human body and vehicle interior

Table 1
Summary of crash characteristics and resulting injury outcomes. Cases were categorized by the presence of AIS 2+ chest soft tissue injury.

	Case Name	Vehicle	AIS Code – Injury Description	Age	Gender	Height (cm)	Weight (kg)	Delta-V (km/h)	Object Struck
Thoracic Soft Tissue Injuries	Escape	2012 Ford Escape	450203.3 - Rib Fracture (L3-4, R5-7,10) 442200.3 - Right Hemothorax 450804.2 - Sternum Fracture	86	M	175	84	49.9	Vehicle
	Cobalt	2006 Chevrolet Cobalt	441406.3 - Left Pneumothorax / Lung Contusion	80	M	183	77	42.6	Vehicle
	Camry	2010 Toyota Camry	442208.2 - Hemomediastinum	21	F	160	64	64	Vehicle
	Cavalier	2002 Chevrolet Cavalier	442202.3 - Pneumothorax	18	M	175	64	49.4	Vehicle
	Hummer	2007 Hummer H3	450203.3 - Rib Fracture (R 3-9) 441402.3 - Bilateral Pulmonary Contusion 450804.2 - Sternum Fracture	50	F	173	86	57.4	Vehicle
Non-Injuries	Solara	2007 Toyota Solara	450202.2 - Bilateral 3rd rib fracture 450804.2 - Sternum fracture	50	F	173	67	31.8	Vehicle
	Corolla	2007 Toyota Corolla		57	M	165	71	54.5	Vehicle
	Civic	2012 Honda Civic		67	F	165	66	56.3	Tree
	Lexus	2008 Lexus ES350		43	M	175	88	69.7	Vehicle
	Malibu	2006 Chevrolet Malibu	450804.2 - Sternum fracture 441004.1 - Minor heart contusion	69	M	173	82	61.1	Vehicle
	Silverado	2005 Chevrolet Silverado		23	M	175	79	59.9	Concrete Wall

models [15, 16]. The original SVM model was developed as an average representation of vehicle interiors across an entire fleet of vehicles using laser scan data from 15 vehicles [16]. Finite element simulations were solved using LS-Dyna r6.1.1 on a cluster computer. Each case reconstruction was performed in an automated fashion involving a three step process previously outlined [14, 17].

First, the frontal crash response of the SVM was tuned to perform similarly to the mechanics of a sister or clone of the vehicle model involved in each reconstructed MVC [18]. For each case, the HIII FEM (Humanetics, Plymouth, MI) was positioned in the SVM according to a frontal New Car Assessment Program (NCAP) report. Up to 10 mechanical restraint properties of the SVM (e.g. seat, seat belt, airbags) were varied using a 120-sample Latin Hypercube design (LHD) of experiments [14, 17]. The set of mechanical parameters yielding the most similar crash response, according to a Sprague and Geers analysis [17, 19], were used as the specific tuned SVM.

In the second phase, THUMS v4.01 was scaled, modified, and positioned within the specific tuned SVMs to model the MVC case occupant using the details found in the CIREN or NASS-CDS databases. The nodal coordinates of THUMS were isometrically scaled. An element deletion model for rib fracture was implemented in THUMS. The mechanical response effects of occupant aging were modeled in the rib cage by modifying the ultimate plastic strain fracture threshold (ε) of cortical rib bone and the cortical bone thickness (t) based on relationships (Equations 1 and 2) used in previous reconstructions of MVCs using THUMS [20-22]. The THUMS model was positioned within the tuned SVM according to data from the CIREN or NASS-CDS case report. For each simulation, the occupant was positioned according to the reported longitudinal seat track position, seat back angle, d-ring anchor height, steering column position, and steering column angle.

$$\varepsilon = (-383 * \text{age(yrs)} + 37514) / 10^6 \quad \text{(Equation 1)}$$

$$t = -0.00578 * \text{age(yrs)} + 1.1335 \quad \text{(Equation 2)}$$

In the final step, the longitudinal event data recorder (EDR) delta-V pulse was extracted from each CIREN or NASS-CDS case. These pulses were used to drive the planar kinematics of the occupant compartment (Figure 1a). Each crash event was simulated for 180 ms.

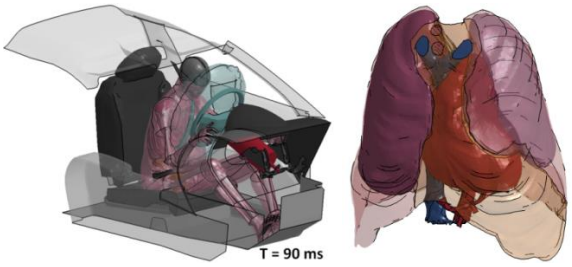

(a) **(b)**

Figure 1. (a) An example crash reconstruction simulation shows the modified THUMS impacting the airbag. (b) The thoracic soft tissue organs of THUMS that were analyzed.

Data Analysis

Several traditional PMHS- and ATD-based chest injury metrics were instrumented in the THUMS v4.01 model and extracted in each simulation [23]. In addition, peak elemental strains in each solid element of each lung were reported and compared to maximum principal strain thresholds for side impact reconstruction cases (0.60), and rat-lung impacts (0.284) existing in literature [11, 12]. The volume fraction of elements exceeding these thresholds were reported in each lung of each simulation.

Stresses and strains were calculated in solid element parts representing the parenchyma of the left and right lungs, the heart, superior vena cava (SVC), inferior vena cava (IVC). Element data was extracted from the shell parts representing the visceral and parietal pleurae, the pericardium, descending aorta, SVC, and IVC (Figure 1b). For each element, the time history of maximum principal strain (ε_{mp}) was evaluated.

The deformation patterns of each element were compared to each other to estimate the degree of similarity between elements using a normalized cross-correlation (NCC) algorithm. By using normalized cross correlation algorithms, the magnitude of the response signal is not evaluated. Instead, the dynamic shape patterns of the tissue deformations are categorized and elements deforming in similar or different temporal patterns can be identified.

The NCC algorithm yields a metric for similarity ranging from 0 to 1, with 0 being no-match and 1 being a perfect match. Software was developed to calculate NCC and perform the following algorithm for each pair of elements in a given part or structure. Elements with the NCC values greater than a pre-selected threshold (0.95 for ε_{mp}) were identified and grouped together [24]. Initially, each element was assigned a pattern ID and characteristic NCC, the latter being the maximum NCC value between itself and the previous elements analyzed. At the beginning of the algorithm, the first element was taken as the template element with an initial pattern ID of 1 and characteristic NCC value of 0. The pattern ID and characteristic NCC were iteratively updated by calculating the NCC between the template element and all remaining comparison elements [24]. The comparison element was grouped with the current template if its NCC was greater than the threshold and greater than the NCCs with previous template elements. Once all remaining elements were compared to the current template, the next element in the part or structure was taken as the current template and the comparison process was repeated until the NCC for each element in the part was calculated. Elements with similar stress profiles were identified and assigned a unique pattern ID. Only patterns with at least 8 member elements were considered in the subsequent analyses for extensive and focal injury mechanisms.

To identify potential regions of extensive injury, such as pulmonary or cardiac contusion, groups of elements that fell into the same pattern ID, and accounted for greater than 5% of the structure volume were analyzed. The pattern group with the greatest average peak ε_{mp} values across all elements in the group were identified in the heart and right and left lungs.

RESULTS

The peak chest deflection, peak sternum acceleration, and lung volume fractions exceeding ε_{mp} thresholds for each simulation are summarized in Table 2. Two tailed student's t-tests were performed on these metrics for the thoracic soft tissue injury cases compared to the non-injurious cases. The chest deflection of the injurious cases was 36.7±3.3 (mean ± 1 standard deviation), while the chest deflection in non-injurious cases was 37.4±6.0. There was no statistically significant difference in the group's chest deflections (p=0.84). The sternum acceleration of the injurious cases was 51.8±10.2, while the sternum acceleration in non-injurious cases was 60.4±13.0. There was also no statistically significant difference in the group's sternum accelerations (p=0.26). None of the peak lung element fraction metrics had statistically significant differences between the two groups (for left lung $\varepsilon_{mp} > 0.284$, p = 0.12, for right lung $\varepsilon_{mp} > 0.284$, p = 0.44, for left lung $\varepsilon_{mp} > 0.60$, p = 0.42, for right lung $\varepsilon_{mp} > 0.60$, p = 0.91).

Table 2
Summary of the injury metrics evaluated in the thoracic region to evaluate soft tissue injury. Rows of green text included pulmonary contusion while the blue text indicates cases with more focal injury events.

	Case	Peak Chest Deflection (mm)	Sternum Acceleration (G's)	Lung Volume Fraction $\varepsilon_{mp} > 0.284$ (Gayzik et al)		Lung Volume Fraction $\varepsilon_{mp} > 0.60$ (Danelson, Stitzel)		Largest Hotspot Average ε_{mp}		
				Left	Right	Left	Right	L Lung	R Lung	Heart
Soft Tissue Injuries	Escape	35.1	38.0	64.1	22.0	2.2	0.2	0.43	0.27	0.34
	Cobalt	35.8	48.9	74.2	30.4	3.1	0.0	0.46	0.30	0.36
	Camry	38.0	66.2	88.3	85.1	15.1	3.3	0.58	0.42	0.42
	Cavalier	33.0	51.1	68.5	54.5	2.8	1.1	0.43	0.47	0.38
	Hummer	41.7	54.7	77.0	66.6	4.4	0.8	0.51	0.40	0.43
Non-Injuries	Solara	31.2	54.7	87.3	58.0	9.5	0.2	0.57	0.34	0.36
	Corolla	44.8	54.1	82.8	66.5	9.4	1.2	0.50	0.39	0.40
	Civic	33.1	74.5	83.4	37.4	4.4	0.0	0.52	0.44	0.38
	Lexus	40.0	78.4	77.9	73.4	6.7	1.4	0.45	0.32	0.34
	Malibu	32.0	45.4	72.7	58.8	2.2	0.6	0.44	0.39	0.34
	Silverado	43.4	55.2	88.2	75.3	17.8	2.7	0.60	0.45	0.45

The injury metrics related to the hotspot analyses using the ε_{mp} time-histories also did not yield any statistically significant differences between the injurious and non-injurious cases at the $p<0.05$ level. The largest hotspot's average ε_{mp} for the left lung ($p=0.43$), right lung ($p=0.70$) and heart ($p=0.76$) parts were not significantly different between injurious and non-injurious cases.

DISCUSSION

While no statistically significant relationships were identified to distinguish between the five thoracic soft tissue injury cases and the six non-injurious cases in the study, important methods have been developed to help quantify the dynamic response of soft tissues that may enlighten injury mechanisms using FEMs in the future. This study analyzed the dynamic response behavior of over 200,000 elements of the chest in THUMS v4.01 and considered their response behavior in relation to neighboring elements and anatomical parts. It should be noted that, despite a lack of statistical significance between injury/non-injury groups, there was more similarity between the sternum acceleration ($p=0.26$) and chest deflection ($p=0.84$) injury metrics than there was with the dynamic response injury metrics evaluated in this study.

At present, several challenges limited the conclusions of this study. In studies where the human body models have been modified to further simulate subject specific characteristics, the hotspot analysis methods may become more sensitive to injury prediction. In the future, the morphology and bone quality of a specific occupant's thoracic anatomy may be implemented into the FEM using morphing techniques with the reported CIREN radiology as a data source. Another difficulty in developing injury metrics using MVC FEM reconstructions with strong correlations will be to identify enough detailed cases that fit the criteria for reconstruction or to develop additional reconstruction methods to account for variability that is not currently modeled in these reconstructions.

CONCLUSIONS

This study evaluated the dynamic response behavior of over 200,000 elements of the thorax in THUMS v4.01 in 11 full frontal crash reconstruction simulations and attempted to quantify soft tissue injury mechanisms. Multiple detailed HBMs incorporate organ level detail with validated tissue mechanical properties. As the level of modeling and analysis methods continue to improve, the use of human body FEMs and data from CIREN and NASS-CDS may allow the injury biomechanics community to evaluate soft tissue injury

mechanisms and physiologic responses that would otherwise be difficult to evaluate in the laboratory. Additionally, the data generated from these injury analyses could be used to further validate and improve the overall response of future HBMs.

ACKNOWLEDGEMENTS

Funding for this project was provided by Toyota's Collaborative Safety Research Center. Views expressed are those of the authors and do not represent the views of any of the sponsors. Computations were performed on the Wake Forest University DEAC Cluster, a centrally managed resource with support provided in part by the University, and the Bridges and Blacklight systems at the Pittsburgh Supercomputing Center (PSC). The authors would like to thank Ryan Barnard for his technical contributions and Johan Iraeus and Mats Lindquist for the SVM. The Authors also thank Logan Miller, Ian Marcus, Mireille Kelley, Xin Ye, Jeff Suhey, Ryan Shannon, Lian Shen, Nathan Hagstrom, and Lucas Coelho for their contributions to the case reconstructions.

REFERENCES

[1] Cavanaugh JM. The biomechanics of thoracic trauma. Accidental Injury: Springer; 1993. p. 362-90.

[2] Ruan J, El-Jawahri R, Chai L, Barbat S, Prasad P. Prediction and analysis of human thoracic impact responses and injuries in cadaver impacts using a full human body finite element model. *Stapp Car C*. 2003;**47**:299-321.

[3] Shorr RM, Crittenden M, Indeck M, Hartunian SL, Rodriguez A. Blunt thoracic trauma. Analysis of 515 patients. *Annals of surgery*. 1987;**206**:200.

[4] Liman ST, Kuzucu A, Tastepe AI, Ulasan GN, Topcu S. Chest injury due to blunt trauma. *European journal of cardio-thoracic surgery*. 2003;**23**:374-8.

[5] Eppinger R, Sun E, Bandak F, Haffner M, Khaewpong N, Maltese M, et al. Development of improved injury criteria for the assessment of advanced automotive restraint systems–II. *National Highway Traffic Safety Administration*. 1999:1-70.

[6] Kuppa S, Eppinger R. Development of an Improved Thoracic Injury Criterion. *Stapp Car Crash J*. 1998;**42**.

[7] Gayzik FS, Martin, R.S., Gabler, H.C., Hoth, J.J., Duma, S.M., Meredith, J.W., Stitzel, J.D. Characterization of crash-induced thoracic loading resulting in pulmonary contusion. *Journal of Trauma*. 2009;**66**:840-9.

[8] Allen GS, Coates NE. Pulmonary contusion: a collective review. *The American surgeon*. 1996;**62**:895-900.

[9] Cohn SM. Pulmonary contusion: review of the clinical entity. *Journal of Trauma and Acute Care Surgery*. 1997;**42**:973-9.

[10] Gayzik FS, Hoth JJ, Daly M, Meredith JW, Stitzel JD. A finite element-based injury metric for pulmonary contusion: investigation of candidate metrics through correlation with computed tomography. *Stapp Car Crash J*. 2007;**51**:189-209.

[11] Gayzik FS, Hoth JJ, Stitzel JD. Finite element–based injury metrics for pulmonary contusion via concurrent model optimization. *Biomechanics and modeling in mechanobiology*. 2011;**10**:505-20.

[12] Danelson KA, Stitzel JD. Finite element model prediction of pulmonary contusion in vehicle-to-vehicle simulations of real-world crashes. *Traffic injury prevention*. 2015;**16**:627-36.

[13] Raghavendran K, Notter RH, Davidson BA, Helinski JD, Kunkel SL, Knight PR. Lung contusion: inflammatory mechanisms and interaction with other injuries. *Shock (Augusta, Ga)*. 2009;**32**:122.

[14] Gaewsky JP, Weaver AA, Koya B, Stitzel JD. Driver injury risk variability in finite element reconstructions of Crash Injury Research and Engineering Network (CIREN) frontal motor vehicle crashes. *Traffic injury prevention*. 2015;**16**:S124-S31.

[15] Shigeta K, Kitagawa Y, Yasuki T. Development of next generation human FE model capable of organ injury prediction. *Proceedings of the 21st Annual Enhanced Safety of Vehicles*. 2009.

[16] Iraeus J, Lindquist M. Development and Validation of a Generic Finite Element Vehicle Buck model for the Analysis of Driver Rib Fractures in Real Life Nearside Frontal Crashes. 2015.

[17] Jones D, Gaewsky J, Weaver A, Stitzel J. A Semi-Automated Approach to Real World Motor Vehicle Crash Reconstruction Using a Generic Simplified Vehicle Buck Model. *SAE International Journal of Transportation Safety*. 2016;**4**.

[18] Anderson G. Vehicle Year & Model Interchange List (Sisters & Clones List). In: Engineering SS, editor.2013.

[19] Sprague M, Geers T. A spectral-element method for modelling cavitation in transient fluid–structure interaction. *International Journal for Numerical Methods in Engineering*. 2004;**60**:2467-99.

[20] Golman AJ, Danelson KA, Miller LE, Stitzel JD. Injury prediction in a side impact crash using human body model simulation. *Accident Analysis & Prevention*. 2014;**64**:1-8.

[21] Golman AJ, Danelson KA, Stitzel JD. Robust human body model injury prediction in simulated side impact crashes. *Computer Methods in Biomechanics and Biomedical Engineering*. 2016;**19**:717-32.

[22] Stein I, Granik G. Rib structure and bending strength: an autopsy study. *Calcified tissue research*. 1976;**20**:61-73.

[23] Miller L, Gaewsky J, Weaver A, Stitzel J, White N. Regional Level Crash Induced Injury Metrics Implemented within THUMS v4. 01. SAE Technical Paper; 2016.

[24] Wang H, Chen T, Torzilli P, Warren R, Maher S. Dynamic contact stress patterns on the tibial plateaus during simulated gait: a novel application of normalized cross correlation. *Journal of biomechanics*. 2014;**47**:568-74.